LETTERS

Single-stranded DNA-binding protein hSSB1 is critical for genomic stability

Derek J. Richard[1], Emma Bolderson[1], Liza Cubeddu[2,3], Ross I. M. Wadsworth[2], Kienan Savage[1,4], Girdhar G. Sharma[5], Matthew L. Nicolette[6], Sergie Tsvetanov[1], Michael J. McIlwraith[7], Raj K. Pandita[5], Shunichi Takeda[8], Ronald T. Hay[9], Jean Gautier[10], Stephen C. West[7], Tanya T. Paull[6], Tej K. Pandita[5], Malcolm F. White[2] & Kum Kum Khanna[1]

Single-strand DNA (ssDNA)-binding proteins (SSBs) are ubiquitous and essential for a wide variety of DNA metabolic processes, including DNA replication, recombination, DNA damage detection and repair[1]. SSBs have multiple roles in binding and sequestering ssDNA, detecting DNA damage, stimulating nucleases, helicases and strand-exchange proteins, activating transcription and mediating protein–protein interactions. In eukaryotes, the major SSB, replication protein A (RPA), is a heterotrimer[1]. Here we describe a second human SSB (hSSB1), with a domain organization closer to the archaeal SSB than to RPA. Ataxia telangiectasia mutated (ATM) kinase phosphorylates hSSB1 in response to DNA double-strand breaks (DSBs). This phosphorylation event is required for DNA damage-induced stabilization of hSSB1. Upon induction of DNA damage, hSSB1 accumulates in the nucleus and forms distinct foci independent of cell-cycle phase. These foci co-localize with other known repair proteins. In contrast to RPA, hSSB1 does not localize to replication foci in S-phase cells and hSSB1 deficiency does not influence S-phase progression. Depletion of hSSB1 abrogates the cellular response to DSBs, including activation of ATM and phosphorylation of ATM targets after ionizing radiation. Cells deficient in hSSB1 exhibit increased radiosensitivity, defective checkpoint activation and enhanced genomic instability coupled with a diminished capacity for DNA repair. These findings establish that hSSB1 influences diverse end-points in the cellular DNA damage response.

Ionizing radiation and anti-cancer drugs can induce DNA DSBs, which are highly cytotoxic lesions. In the S and G2 phases of the cell cycle, homologous recombination can be used to repair DSBs. To initiate homologous recombination, DNA is resected and then bound by RPA, a eukaryotic SSB, to facilitate Rad51 nucleofilament formation and strand invasion[2]. Here we show that, in addition to RPA, the human genome encodes two further conserved SSB homologues, present on chromosomes 12q13.3 and 2q32.3, which we have named hSSB1 and hSSB2, respectively. The main focus of this study, hSSB1, is highly represented in EST libraries from a variety of tissues. It is conserved in metazoa, comprising an amino-terminal oligonucleotide/oligosaccharide-binding-fold domain, followed by a more divergent carboxy-terminal domain (Supplementary Fig. 1). Like RPA, recombinant hSSB1 binds specifically to ssDNA substrates (Fig. 1a and Supplementary Fig. 2), in particular to

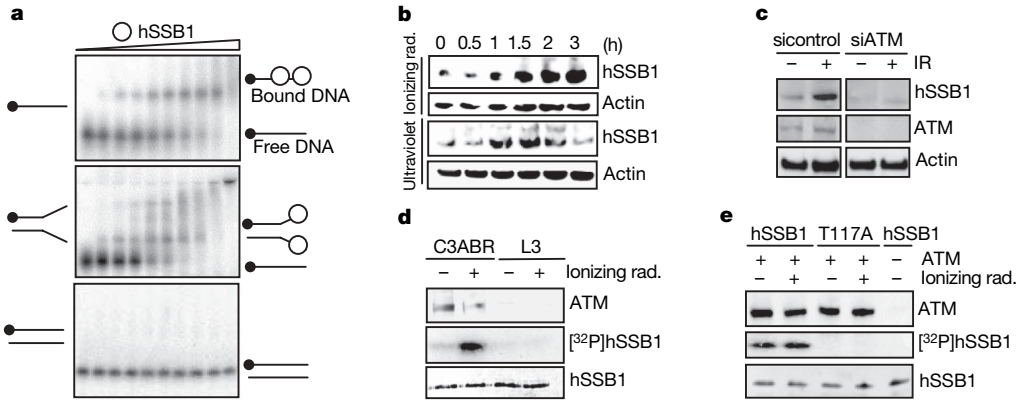

Figure 1 | ATM-dependent stabilization and phosphorylation of hSSB1 after ionizing radiation. a, Electrophoretic mobility shift analysis showing binding of recombinant hSSB1 to ssDNA substrates, d30T (top), a synthetic replication fork (middle) and dsDNA (bottom). The radiolabel is marked with a black circle. **b**, Immunoblots of hSSB1 using cell extracts from neonatal foreskin fibroblasts (NFFs) exposed to ionizing (6 Gy) or ultraviolet (20 J m^{-2}) radiation. Cells were harvested at the indicated time points and immunoblotted for hSSB1. **c**, Western blots of hSSB1 using ionizing radiation-treated (6 Gy) extracts from NFFs transfected with ATM siRNA. **d**, ATM was immunoprecipitated from mock or ionizing radiation (6 Gy)-treated normal (C3ABR) and A-T (L3) cell lines. *In vitro* kinase assays were performed using recombinant hSSB1 as a substrate. **e**, Phosphorylation of hSSB1 (number denotes the position of threonine residue substituted with alanine) by immunoprecipitated ATM kinase.

[1]Signal Transduction Laboratory, Queensland Institute of Medical Research, Brisbane, Queensland 4029, Australia. [2]Centre for Biomolecular Sciences, University of St Andrews, North Haugh, St Andrews, Fife KY16 9ST, UK. [3]School of Molecular and Microbial Biosciences, University of Sydney, Sydney, New South Wales 2006, Australia. [4]Central Clinical Division, School of Medicine, University of Queensland, Queensland 4072, Australia. [5]Department of Radiation Oncology, Washington University School of Medicine, St Louis, Missouri 63108, USA. [6]Department of Molecular Genetics and Microbiology, University of Texas at Austin, Austin, Texas 78712, USA. [7]London Research Institute, Clare Hall Laboratories, Cancer Research UK, South Mimms, Hertfordshire EN6 3LD, U.K. [8]Department of Radiation Genetics, Kyoto University Graduate School of Medicine, Kyoto 606-8501, Japan. [9]Division of Gene Regulation and Expression, Wellcome Biocentre, University of Dundee, Dundee DD1 5EH, U.K. [10]Institute for Cancer Genetics, Columbia University Medical Center, New York, New York 10032, USA.

polypyrimidines (Supplementary Fig. 3). The binding affinity increases significantly with the length of the DNA substrate (Supplementary Fig. 4).

RPA has several functions in the cell, including roles in DNA replication, recombination and repair[1]. To investigate if hSSB1 functions in similar pathways, we analysed the response of hSSB1 to DNA damage. Cells were treated with ionizing or ultraviolet radiation, and hSSB1 was detected by western blotting (see Supplementary Fig. 5 for protein purification, short interfering RNA (siRNA)-mediated knockdown and antibody characterization). We found that hSSB1 accumulated in the cell in response to DNA damage (Fig. 1b), and that this was due to protein stabilization as treatment with the proteosome inhibitor MG132 led to a similar stabilization (Supplementary Fig. 6).

ATM kinase activity is essential for cellular signalling in response to DNA breaks[3]. siRNA-mediated depletion of ATM, inhibition of ATM activity (wortmannin treatment) or deficiency of ATM in ataxia telangiectasia (A-T) cells resulted in an inability to stabilize hSSB1 after ionizing radiation (Fig. 1c and Supplementary Fig. 7). Co-immunoprecipitation and glutathione *S*-transferase (GST)–ATM fragment[4] pull-down assays indicated that interaction between hSSB1 and ATM was direct and mediated by ATM fragment 4 (amino acids 772–1102) (Supplementary Figs 8 and 9).

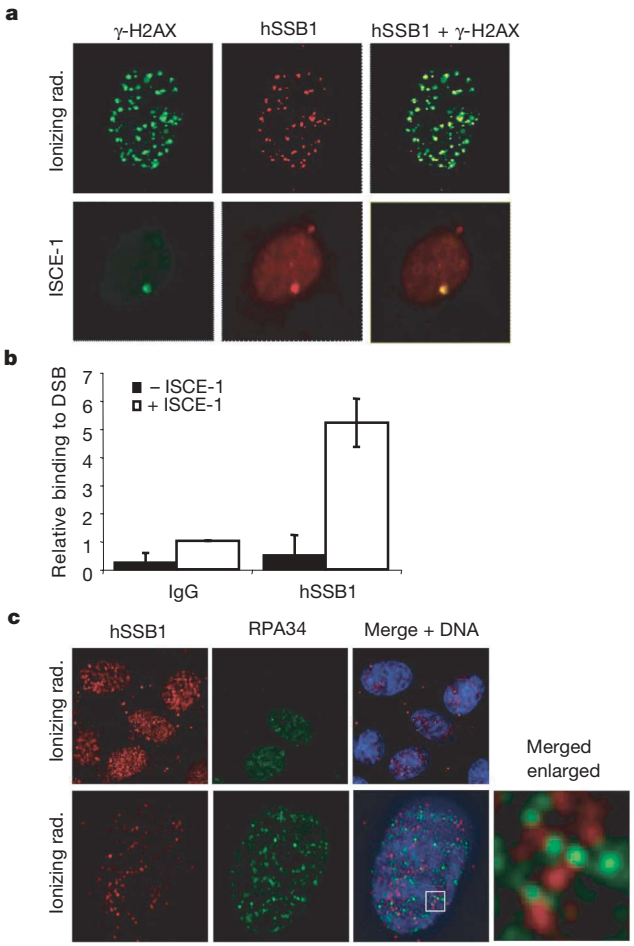

Figure 2 | hSSB1 localizes to DNA repair foci after ionizing radiation. **a**, Irradiated (6 Gy) NFFs were extracted with detergent before fixation and stained with anti-hSSB1 and anti-γH2AX antibodies (top panel; Leica TCS BI-15 microscope). hSSB1 and γ-H2AX co-localize at a single DSB induced by the *I-SceI* restriction enzyme in MCF7 DRGFP cells[7] (bottom panel; Olympus BX61 microscope). **b**, ChIP analysis of hSSB1 on a unique DSB induced by *I-SceI in vivo*. Real-time PCR on ChIP samples used primers directed at 94–378 nucleotides from the DSB[8]. The enrichment of hSSB1 after induction of the DSB was compared with that of an IgG control (±s.d., $n = 3$). **c**, hSSB1 and RPA34 foci do not co-localize. NFFs were irradiated and 2 h later fixed and stained with anti-hSSB1 and anti-RPA34 antibodies. Images were acquired using Deltavision Personal DV. An enlargement of the merged image is displayed, demonstrating proximity of hSSB1 and RPA foci.

ATM phosphorylates several proteins involved in the DNA damage-response pathway[3]. *In vitro* kinase assays[5] showed that hSSB1 was a substrate of ATM (Fig. 1d) and that the phosphorylation site was mapped to T117 because mutation of the threonine to alanine blocked phosphorylation by ATM (Fig. 1e). To determine the functional relevance of this phosphorylation site *in vivo*, we compared the expression levels of exogenous GFP-hSSB1 wild-type and T117A mutant in HeLa cells. After ionizing radiation treatment, stabilization was only observed for the wild-type protein (Supplementary Fig. 10a), confirming the role of ATM in ionizing-radiation-induced stabilization. The stabilization defect is unlikely to be due to incorrect folding because recombinant T117A hSSB1 mutant folds correctly and shows similar ssDNA binding as wild-type hSSB1 (Supplementary Fig. 11a, b). Furthermore, GFP-hSSB1 and T117A were rapidly stabilized in the presence of MG132, whereas T117E mutant was not. This indicates that phosphorylation of hSSB1 at T117 prevents its degradation by the proteosome (Supplementary Fig. 10b).

After exposure to ionizing radiation, many repair proteins, including γ-H2AX, localize rapidly to sites of damage[6]. Immunofluorescence showed that hSSB1 localizes to prominent nuclear foci that formed within 30 min of DNA damage and persisted up to 8 h (Fig. 2a and data not shown). Foci for hSSB1 co-localized with most γ-H2AX foci after ionizing radiation and at a single *I-SceI*-induced DSB[7] (Fig. 2a). Unlike hSSB1, we failed to observe significant co-localization of ionizing-radiation-induced RPA and γ-H2AX foci (Supplementary Fig. 12). Chromatin immunoprecipitation[8] revealed that hSSB1 is present close (94–378 base pairs) to the *I-SceI*-induced DSB, suggesting that it might have a direct role in DSB repair (Fig. 2b).

The observation that hSSB1, like RPA, is recruited to sites of DSBs raises the issue of how these proteins are coordinated. RPA forms foci at sites of DNA replication in unperturbed S phase and after DNA damage both in S- and G2-phase cells[9,10]. We examined whether hSSB1 exhibited similar foci formation kinetics and cell-cycle dependence. Before exposure to ionizing radiation, 22% of cells were positive for RPA foci, increasing to about 40% 3 h after treatment. By contrast, there were very few cells (less than 5%) positive for hSSB1 foci before exposure to ionizing radiation. However, 30 min after exposure, more than 95% of cells contained hSSB1 foci. Therefore, unlike RPA, hSSB1 foci formation is not cell-cycle dependent. In cells that contained both RPA and hSSB1 foci, we observed little co-localization (less than 5%), although it is interesting to note that about 27% of RPA foci were in close proximity to hSSB1 (less than 50 nm) (Fig. 2c). This proximity may represent different sub-compartments within one repair centre or a snapshot of the temporally dynamic composition of foci[11]. The lack of direct co-localization indicates functional differences between these proteins in the repair process, although their proximity might suggest that they function at the same sites of repair.

The localization of hSSB1 to repair foci suggests it may act directly in DNA repair or in ionizing-radiation-induced signalling events. In response to DSBs, the cell cycle is arrested, before progression into S phase (G1/S checkpoint) or commitment to mitosis (G2/M checkpoint)[3]. These arrests are eventually released when the DNA lesions have been repaired. To determine whether hSSB1 was involved in checkpoint activation, we examined the effects of hSSB1 depletion on the activation of G1/S[12] and G2/M[13] checkpoints after ionizing radiation. Unlike RPA[14], depletion of hSSB1 by siRNA (sihSSB1) did not influence the number of cells in S phase or progression through it (Supplementary Fig. 13). Although control siRNA-treated cells arrest in G1 and G2 in response to ionizing radiation, hSSB1-depleted cells failed to arrest at either checkpoint (Fig. 3a and Supplementary Fig. 14). Cdc25a, a marker for rapid G1 arrest[15], is normally degraded

after ionizing radiation, but in hSSB1-deficient cells Cdc25a levels remained stable (Supplementary Fig. 15). The ATM-mediated phosphorylation of many checkpoint proteins is vital for ionizing-radiation-induced checkpoint activation[3]. To determine if this cascade was functional in the absence of hSSB1, we analysed the phosphorylation status of several ATM substrates in hSSB1-deficient cells. As expected, irradiation of control cells led to the autophosphorylation of ATM, phosphorylation of p53, Chk2, Chk1 and NBS1 (Fig. 3b). By contrast, hSSB1-deficient fibroblasts failed to show a similar degree of ATM autophosphorylation and phosphorylation of ATM targets after irradiation (Fig. 3b and Supplementary Fig. 16). Furthermore, defective phosphorylation of Chk1 also suggests a function of hSSB1 in ATR-dependent signalling.

Like hSSB1, the MRN complex plays a crucial role in the regulation of ATM activation and activity. We therefore determined whether hSSB1 affects MRN-dependent regulation of ATM activity[16]. We found that wild-type hSSB1 had no effect on ATM activity, whereas the phospho-mimic mutant consistently increased activity by more than twofold, 2.3 ± 0.71 (s.e.m., $n = 3$) (Fig. 3c). hSSB1 itself was not phosphorylated in this assay owing to the vast molar excess of p53. These results suggest that, once ATM is activated, a positive feedback loop is initiated through phosphorylated hSSB1, which in turn reinforces ATM activation. ATM signalling was examined in cells expressing GFP-hSSB1, T117A and T117E. Intriguingly, the expression of T117A suppressed ATM activation, as measured by S1981 phosphorylation, whereas the phospho-mimic T117E enhanced phosphorylation by approximately twofold (Fig. 3d). Together, these results indicate that hSSB1 amplifies ATM-dependent signalling.

Given that ATM is crucial for cell survival after ionizing radiation, we next examined the sensitivity of hSSB1-deficient cells to ionizing radiation. Cells deficient in hSSB1 displayed hypersensitivity to ionizing radiation (Fig. 4a). We were unable to assess cell survival after longer time points because of the severe death phenotype exhibited by ionizing radiation-treated hSSB1-deficient cells. Indeed, we usually observed greater than 90% cell death within 96 h of exposure to very low doses of radiation (0.5 Gy). Furthermore, we found that even depletion of hSSB1 by 50% resulted in ionizing radiation sensitivity (Supplementary Fig. 17). Cells deficient in hSSB1 also displayed higher frequencies of chromosomal aberrations (chromosome and chromatid breaks, with fragments and telomere fusions) after exposure to ionizing radiation (Fig. 4b and Supplementary Fig. 18). These findings demonstrate that hSSB1 plays a functionally important role in allowing cells to repair genotoxic damage and maintain chromosome stability.

Because SSBs are required for homologous recombination[17], we determined whether hSSB1 was important for homologous recombination in human cells. Depletion of hSSB1 from the MCF7 cell line, stably integrated with a GFP-based homologous recombination reporter construct[7,18], resulted in an approximate fivefold reduction in homologous recombination, as measured by GFP-positive cells after *I-Sce1* expression (Supplementary Fig. 19). Rad51 binds ssDNA at resected DSBs to form nucleoprotein filaments that mediate the invasion of ssDNA into homologous duplex DNA[2]. These reactions are stimulated by the presence of RPA[19,20]. We therefore compared the ability of RPA and hSSB1 to stimulate Rad51-mediated strand invasion. We found that hSSB1 stimulated Rad51-mediated D-loop formation to a similar extent as RPA (Fig. 4c). Wild-type and T117E hSSB1 showed comparable stimulation in this assay, indicating that ATM-dependent hSSB1 phosphorylation does not appear to regulate strand invasion. Like RPA, hSSB1 was unable to stimulate strand invasion when added before Rad51 (data not shown). The stimulation of Rad51-mediated strand invasion by hSSB1 is likely to occur by a mechanism similar to that described previously with RPA[21,22]. Consistent with these findings, Rad51 was not recruited to foci after ionizing radiation in hSSB1-deficient cells (Supplementary Fig. 20). Rad51 and hSSB1 were found to co-localize in 12% of cells treated with ionizing radiation, an additional 14% of foci were proximal (less than 50 nm) (Supplementary Fig. 21). An interaction between hSSB1 and Rad51 was also detected by co-immunoprecipitation (Supplementary Fig. 22).

In summary, we have identified a novel protein, hSSB1, that plays a key role in DNA damage response. Before this study, RPA was

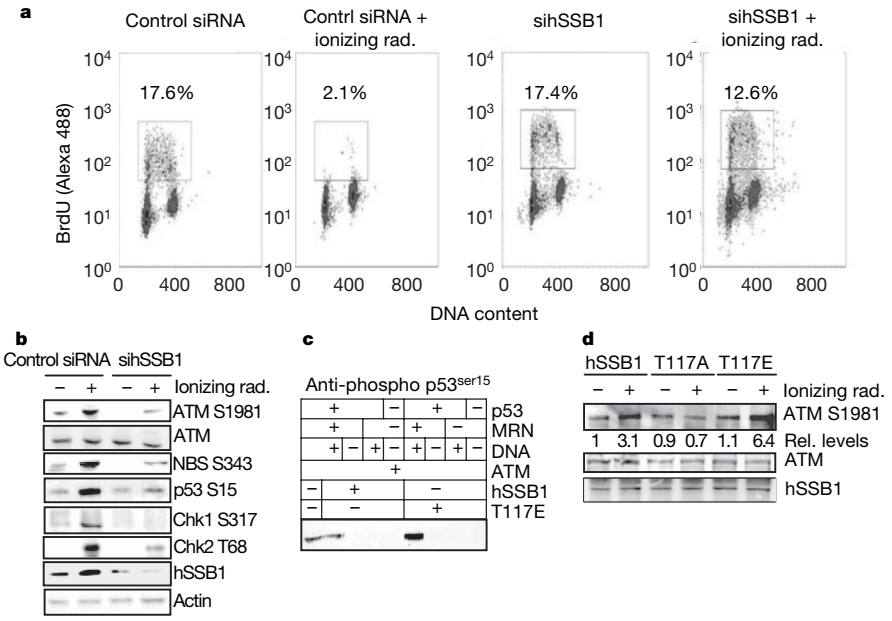

Figure 3 | hSSB1 inhibition results in defective ionizing-radiation-induced checkpoint activation and defective ATM signalling. a, hSSB1 inhibition results in defective ionizing-radiation-induced G1/S checkpoint. NFFs were mock-treated or irradiated (6 Gy) and labelled with BrdU, stained with anti-BrdU-Alexa488 antibodies and propidium iodide. The percentage of BrdU-positive cells (boxed area) was determined by fluorescence-activated cell sorting. **b**, hSSB1 is required for ionizing-radiation-induced ATM activation and activity. SiRNA-transfected NFFs were treated with ionizing radiation and subjected to immunoblotting with the antibodies indicated. **c**, hSSB1-T117E affects MRN-dependent ATM activity. Purified ATM was incubated with DNA and MRN in the presence of wild-type hSSB1 or T117E mutant; phosphorylation of GST-p53 was detected using anti-Ser15 p53 antibody. **d**, hSSB1-T117E induces hyperactivation of ATM. HeLa cells transiently transfected with the indicated constructs were treated with ionizing radiation and immunoblotted with the antibodies indicated.

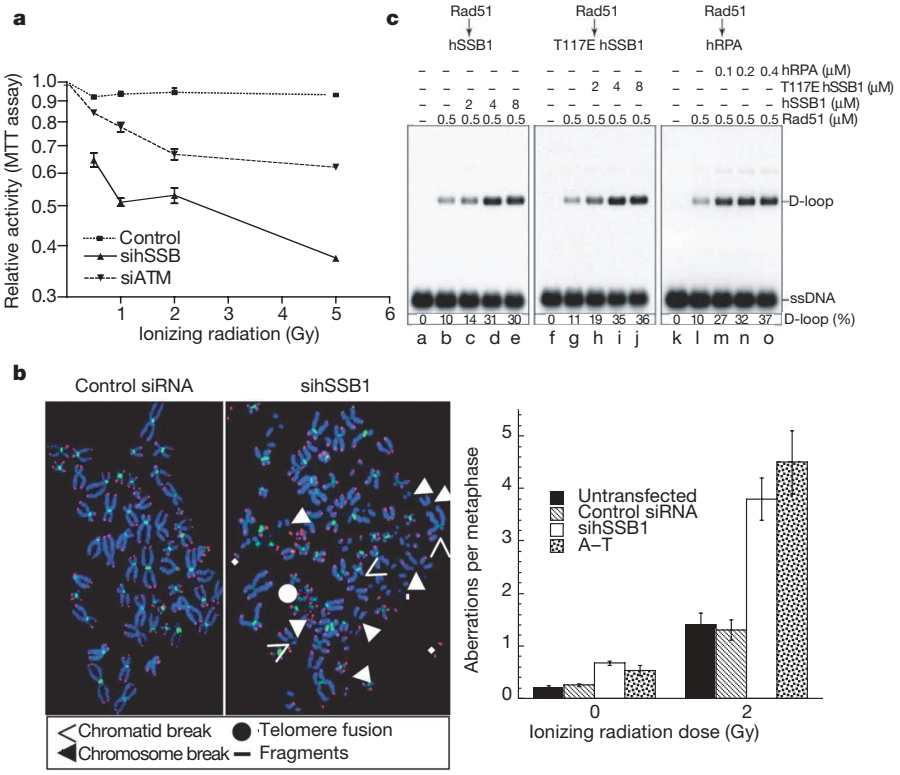

Figure 4 | hSSB1 is required for efficient DNA repair. a, hSSB1-depleted cells are hypersensitive to ionizing radiation. NFFs were treated with siRNAs before treatment with the indicated ionizing radiation doses. Cells were allowed to grow for 36 h before metabolism was measured by the MTT assay (±s.e.m., $n = 3$). **b**, Representative metaphase spreads of irradiated control and hSSB1-deficient cells. Telomeres (red) and centromeres (green) are labelled[27]; chromosome breaks are indicated by arrowheads. Frequencies of spontaneous and ionizing-radiation-induced (2 Gy) chromosome, as well as chromatid, breaks and fragments in siRNA-transfected and AT cells, used as positive control, are indicated (±s.d., $n = 3$). Fifty metaphases for each sample were analysed. **c**, hSSB1 stimulates Rad51-dependent strand exchange. Strand-invasion recombination reactions were performed between ^{32}P-end-labelled linear ssDNA and homologous supercoiled plasmid DNA using Rad51, hSSB1 and RPA as indicated.

thought to be the sole functional homologue of the SSBs in the nucleus of mammalian cells. However, the discovery of a second SSB (hSSB1) in metazoa indicates that higher eukaryotes have preserved this family of proteins in a simpler molecular configuration more closely related to crenarchaeal SSB[23]. Our studies provide new insights into mechanisms of DNA-damage signal transduction and reveal that hSSB1 influences diverse endpoints in the cellular DNA damage response, including cell-cycle checkpoint activation, recombinational repair and maintenance of genomic stability. Our data demonstrate that hSSB1 associates with DNA lesions, and enables the efficient activation of ATM and consequent phosphorylation of downstream proteins. It also promotes Rad51-mediated strand exchange and may thus contribute directly to homologous recombination repair. Finally, as an early participant in the damage-response pathway[24], hSSB1 may also be involved in preventing tumorigenesis and might affect the response of patients and tumours towards radiotherapy and DNA-damaging chemotherapies.

METHODS SUMMARY

Chromatin immunoprecipitation (ChIP) assays were performed as described previously[8,25]. MTT (3-(4,5-dimethylthiazol-2-yl)-2,5-diphenyltetrazolium bromide) assays were performed essentially as described by Slavotinek *et al.*[26] with the exception that assays were performed 36 h after ionizing radiation treatment. G1/S checkpoint was measured using bromodeoxy uridine (BrdU) incorporation assay[12], and G2/M checkpoint by labelling cells with anti-phospho-histone H3 antibody[13] as described previously. To analyse chromosome aberrations at metaphase, exponentially growing cells were treated with 2 Gy of ionizing radiation, colcemid added at different time points, metaphase cells collected and chromosome aberrations scored as described[27]. The effect of hSSB1 on MRN-dependent activation of ATM was determined as described previously[16]. Homologous recombination was measured by determining the frequency of reconstitution of a green fluorescent protein reporter gene (*pDR-GFP*) within a chromosomally integrated plasmid substrate in cells, as described previously[7,18].

Full Methods and any associated references are available in the online version of the paper at www.nature.com/nature.

Received 21 December 2007; accepted 3 March 2008.
Published online 30 April 2008.

1. Wold, M. S. Replication protein A: a heterotrimeric single-stranded DNA-binding protein required for eukaryotic DNA metabolism. *Annu. Rev. Biochem.* **66**, 3050–3059 (1997).
2. West, S. C. Molecular views of recombination proteins and their control. *Nature Rev. Mol. Cell Biol.* **4**, 435–445 (2003).
3. Khanna, K. K. & Jackson, S. P. DNA double-strand breaks: signaling, repair and the cancer connection. *Nature Genet.* **27**, 247–254 (2001).
4. Khanna, K. K. *et al.* ATM associates with and phosphorylates p53: mapping the region of interaction. *Nature Genet.* **20**, 398–400 (1998).
5. Gatei, M. *et al.* Role for ATM in DNA damage-induced phosphorylation of BRCA1. *Cancer Res.* **60**, 3299–3304 (2000).
6. Bekker-Jensen, S. *et al.* Spatial organization of the mammalian genome surveillance machinery in response to DNA strand breaks. *J. Cell Biol.* **173**, 195–206 (2006).
7. Pierce, A. J., Johnson, R. D., Thompson, L. H. & Jasin, M. XRCC3 promotes homology-directed repair of DNA damage in mammalian cells. *Genes Dev.* **13**, 2633–2638 (1999).
8. Rodrigue, A. *et al.* Interplay between human DNA repair proteins at a unique double-strand break *in vivo*. *EMBO J.* **25**, 222–231 (2006).
9. Jazayeri, A. *et al.* ATM- and cell cycle-dependent regulation of ATR in response to DNA double-strand breaks. *Nature Cell Biol.* **8**, 37–45 (2006).
10. Soutoglou, E. *et al.* Positional stability of single double-strand breaks in mammalian cells. *Nature Cell Biol.* **9**, 675–682 (2007).
11. Lisby, M., Barlow, J. H., Burgess, R. C. & Rothstein, R. Choreography of the DNA damage response: spatiotemporal relationships among checkpoint and repair proteins. *Cell* **16**, 328–334 (2004).

12. Fabbro, M. *et al.* BRCA1-BARD1 complexes are required for p53Ser-15 phosphorylation and a G1/S arrest following ionising radiation-induced DNA damage. *J. Biol. Chem.* **279,** 31251–31258 (2004).
13. Xu, B., Kim, S. T. & Kastan, M. B. Involvement of Brca1 in S-phase and G(2)-phase checkpoints after ionising irradiation. *Mol. Cell. Biol.* **21,** 3445–3450 (2001).
14. Dodson, G. E., Shi, Y. & Tibbetts, R. S. DNA replication defects, spontaneous DNA damage, and ATM-dependent checkpoint activation in replication protein A-deficient cells. *J. Biol. Chem.* **279,** 34010–34014 (2004).
15. Mailand, N. *et al.* Rapid destruction of human Cdc25A in response to DNA damage. *Science* **288,** 1425–1429 (2000).
16. Lee, J. H. & Paull, T. T. ATM activation by DNA double-strand breaks through the Mre11-Rad50-Nbs1 complex. *Science* **308,** 551–554 (2005).
17. Wang, Y. *et al.* Mutation in *Rpa1* results in defective DNA double-strand break repair, chromosomal instability and cancer in mice. *Nature Genet.* **37,** 750–755 (2002).
18. Zhang, J., Ma, Z., Treszezamsky, A. & Powell, S. N. MDC1 interacts with Rad51 and facilitates homologous recombination. *Nature Struct. Mol. Biol.* **12,** 902–909 (2005).
19. McIlwraith, M. J. *et al.* Reconstitution of the strand invasion step of double-strand break repair using human RAD51, RAD52 and RPA proteins. *J. Mol. Biol.* **304,** 151–164 (2000).
20. Song, B. W. & Sung, P. Functional interactions among yeast Rad51 recombinase, Rad52 mediator, and replication protein A in DNA strand exchange. *J. Biol. Chem.* **275,** 15895–15904 (2000).
21. New, J. H. & Kowalczykowski, S. C. Rad52 protein has a second stimulatory role in DNA strand exchange that complements replication protein-A function. *J. Biol. Chem.* **277,** 26171–26176 (2002).
22. Sugiyama, T. & Kowalczykowski, S. C. Rad52 protein associates with replication protein A (RPA)-single-stranded DNA to accelerate Rad51-mediated displacement of RPA and presynaptic complex formation. *J. Biol. Chem.* **277,** 31663–31672 (2002).
23. Wadsworth, R. I. & White, M. F. Identification and properties of the crenarchaeal single-stranded DNA binding protein from *Sulfolobus solfataricus. Nucleic Acids Res.* **29,** 914–920 (2001).
24. Bartkova, J. *et al.* DNA damage response as a candidate anti-cancer barrier in early human tumorigenesis. *Nature* **434,** 864–870 (2005).
25. Aparicio, O. *et al.* in *Current Protocols in Molecular Biology* (eds Ausubel, F. A. *et al.*) 21.3.1–21.3.17 (John Wiley, New York, 2005).
26. Slavotinek, A., McMillan, T. J. & Steel, C. M. Measurement of radiation survival using the MTT assay. *Eur. J. Cancer* **30,** 1376–1382 (1994).
27. Pandita, R. K. *et al.* Mammalian Rad9 plays a role in telomere stability, S- and G2-phase-specific cell survival, and homologous recombinational repair. *Mol. Cell. Biol.* **26,** 1850–1864 (2006).

Supplementary Information is linked to the online version of the paper at www.nature.com/nature.

Acknowledgements This study was supported by grants from the National Health and Medical Research Council of Australia (to K.K.K.), Cancer Research UK (to S.C.W.), the Biotechnology and Biological Sciences Research Council of the UK (to M.F.W), the National Institutes of Health (CA92245 to J.G.; CA10445 and CA123232 to T.K.P.) and the American Cancer Society (RGS-04-173-01-CCG to T.T.P.).

Author Information The genes hSSB1 and hSSB2 are deposited in NCBI under accession numbers NM_024068 and NM_001031716, respectively. Reprints and permissions information is available at www.nature.com/reprints. Correspondence and requests for materials should be addressed to K.K.K. (kumkumK@qimr.edu.au) or M.F.W. (mfw2@st-and.ac.uk).

METHODS

Plasmids and siRNA. Full-length *hSSB1* was amplified by PCR from HeLa-cell complementary DNA and cloned in the *BamH*I and *Sal*I sites of bacterial expression His-tag vector pET28c; *hSSB2* was cloned into bacterial expression His-tag vector pET19b. GFP-hSSB1 fusion protein was cloned into the *Hind*III and *Kpn*I sites of pEGFP-C1, and threonine 117 was mutated to alanine using QuickChange site-directed mutagenesis, as described previously[12].

siRNAs were chemically synthesized (Invitrogen) with a two-nucleotide deoxythymidine overhang at the 3′-end. Individual siRNA sequences were as follows: hSSB1 (sense) 5′-GACAAAGGACGGGCAUGAGdTdT, (antisense) 5′-CUCAUGCCCGUCCUUUGUCdTdT, ATM (sense) 5′-GCGCCUGAUUCG-AGAUCCUdTdT, (antisense) 5′-AGGAUCUCGAAUCAGGCGCdTdT. Cells were transfected twice with siRNA at a 24 h interval and processed 48 h later.

The 100-base oligonucleotide used in the D-loop assay was: 5′-GGGCGAA-TTGGGCCCGACGTCGCATGCTCCTCTAGACTCGAGGAATTCGGTACCCC-GGGTTCGAAATCGATAAGCTTACAGTCTCCATTTAAAGGACAAG-3′. The oligo was 5′-^{32}P-end-labelled using polynucleotide kinase (New England Biolabs) and [γ-^{32}P]ATP.

Purification of recombinant protein. BL21 cells expressing His-tagged hSSB1 were lysed in buffer A (20 mM Tris pH 8.0, 50 mM NaCl and 30 mM imidazole) with the addition of protease inhibitor cocktail (Complete Mini EDTA-free Protease, Roche) and 0.1% Triton X-100. Clarified soluble *E. coli* cell lysate pretreated with DNaseI (30 min, 20 °C) was applied to a Hi-Trap metal chelating column (GE Healthcare) loaded with nickel in buffer A and eluted using a gradient of 0–100% 300 mM imidazole. hSSB1 protein isolated by nickel chromatography was diluted 3× in buffer A with 1 mM DTT and no NaCl, and loaded onto a heparin column (HiTrap, GE Healthcare). Protein was eluted using a gradient of 0–100% 1 M NaCl. hSSB1 was concentrated and re-applied to the gel filtration column (Superdex 200) in buffer B (20 mM Tris pH 8.0, 150 mM NaCl and 1 mM DTT). Fractions were finally pooled, concentrated, snap frozen and stored at –80 °C.

Electrophoretic mobility shift analysis. The interaction of hSSB1 with d30T oligonucleotide was investigated using native acrylamide electrophoretic mobility shift analysis. Increasing concentrations of hSSB1 were incubated with ^{32}P-labelled d30T ssDNA (50 pmol) in buffer (20 mM HEPES, pH 7.3, 100 mM KCl and 1 mM $MgCl_2$, 1 mg μl^{-1} bovine serum albumin) at 20 °C for 30 min in 10 µl total volume. Reactions were resolved on 10% native acrylamide/TBE gel. Gels were exposed to a phosphorimage plate and the image visualized with a Fuji FLA-5000 Phosphoimager.

Isothermal titration calorimetry. Calorimetric experiments used a VP-ITC instrument (MicroCal). All solutions were degassed before use. hSSB1 samples were dialysed extensively against 20 mM HEPES buffer, pH 7.3, 100 mM KCl and 1 mM $MgCl_2$. Oligonucleotides were also dissolved in isothermal titration calorimetry (ITC) buffer. Binding experiments were performed in triplicate at 37 °C. A 370-µl syringe, stirring at 300 r.p.m., was used to titrate the oligonucleotide into the sample cell containing approximately 1.4 ml hSSB1. Each titration consisted of a preliminary 1-µl injection followed by up to 25 subsequent 10-µl injections. Heats of dilution were measured in corresponding blank titrations by adding oligonucleotide to ITC buffer and/or ITC buffer to protein, and were found to be similar to heats observed at the end of protein–DNA titrations. ITC-binding isotherms were analysed using a simple single-binding site model with ITC data analysis software (ORIGIN) provided by the manufacturer.

Antibodies and immunofluorescence. Antibodies used in this study were supplied by Calbiochem (Rad50, Mre11, Rad51), Santa Cruz (Cdc25a), Upstate (γH2AX), Roche (BRDU), Cell Signalling Technologies (pT68-Chk2, pS317-Chk1, pS15-p53), Merck (H3 S10) and Invitrogen (GFP and Alexa secondary antibodies). Sheep antiserum to hSSB1 was raised against full-length recombinant His-tagged hSSB1. For immunofluorescent staining, cells were pre-permeabilized with 20 mM HEPES (pH 8), 20 mM NaCl, 5 mM $MgCl_2$, 1 mM ATP, 0.1 mM N_2OV, 1 mM NaF and 0.5% NP40 for 15 min on ice before fixation in 4% paraformaldehyde (w/v) in PBS for 10 min.

D-loop assay. For D-loop assay, reactions contained 5′-^{32}P-end-labelled 100-base ssDNA (1 µM), and the indicated concentration of Rad51, hSSB1 or RPA in standard buffer (25 mM Tris-acetate pH 7.5, 5 mM $CaCl_2$, 2 mM ATP, 1 mM DTT, 100 µg μl^{-1} bovine serum albumin). Proteins were added and mixed in the sequence indicated. After 5 min at 37 °C, excess supercoiled pPB4.3 DNA (0.3 mM) was added and incubated for 10 min. The products were deproteinized by the addition of one-fifth volume of stop buffer (0.1 M Tris–HCl pH 7.5, 0.1 M $MgCl_2$, 3% SDS and 10 mg μl^{-1} proteinase K) followed by electrophoresis, autoradiography and quantification using a Typhoon Trio PhosphorImager (GE Healthcare).